*Inorg. Chem.* **2006**, *45*, 3004–3013


# Copper–Dioxygen Adducts and the Side-on Peroxo Dicopper(II)/ Bis(μ-oxo) Dicopper(III) Equilibrium: Significant Ligand Electronic Effects

**Lanying Q. Hatcher,[†] Michael A. Vance,[‡] Amy A. Narducci Sarjeant,[†] Edward I. Solomon,[‡] and Kenneth D. Karlin*[,†]**

*Department of Chemistry, The Johns Hopkins University, Baltimore, Maryland 21218, and Department of Chemistry, Stanford University, Stanford, California 94305*

Received December 23, 2005

The variation of ligand para substituents on pyridyl donor groups of tridentate amine copper(I) complexes was carried out in order to probe electronic effects on the equilibrium between $\mu$-$\eta^2$:$\eta^2$-(side-on)-peroxo $[Cu^{II}_2(O_2^{2-})]^{2+}$ and bis($\mu$-oxo) $[Cu^{III}_2(O^{2-})_2]$ species formed upon reaction with $O_2$. $[Cu^{I}(R\text{-PYAN})(MeCN)_n]B(C_6F_5)_4$ (R-PYAN = *N*-[2-(4-R-pyridin-2-yl)-ethyl]-*N,N′,N′*-trimethyl-propane-1,3-diamine, R = $NMe_2$, OMe, H, and Cl) (**1$^{R}$**) vary over a narrow range in their $Cu^{II}/Cu^{I}$ redox potentials ($E_{1/2}$ vs $Fe(cp)_2^{+/0}$ = –0.40 V for **1$^{NMe2}$**, –0.38 V for **1$^{OMe}$**, –0.33 V for **1$^{H}$**, and –0.32 V for **1$^{Cl}$**) and in C–O stretching frequencies of their carbonyl adducts, **1$^{R}$–CO**: $\nu$(C–O) = 2080, 2086, 2088, and 2090 $cm^{-1}$ for R = $NMe_2$, OMe, H, and Cl, respectively. However, within this range of electronic properties for **1$^{R}$**, dioxygen reactivity is significantly affected. The reaction of **1$^{Cl}$** or **1$^{H}$** with $O_2$ at –78 °C in $CH_2Cl_2$ gives UV–vis and resonance Raman spectra indicative of a $\mu$-$\eta^2$:$\eta^2$-(side-on)-peroxo dicopper(II) adduct (**2$^{R}$**). Compound **1$^{OMe}$** reacts with $O_2$, yielding equilibrium mixtures of side-on peroxo (**2$^{OMe}$**) and bis($\mu$-oxo) (**3$^{OMe}$**) species. Oxygenation of **1$^{NMe2}$** leads to the sole generation of the bis($\mu$-oxo) dicopper(III) complex (**3$^{NMe2}$**). A solvent effect was also observed; in acetone or THF, increased ratios of bis($\mu$-oxo) relative to side-on peroxo complex are observed. Thus, the equilibrium between a dicopper side-on peroxo and bis($\mu$-oxo) species can be tuned by ligand design—specifically, more electron donating ligands favor the formation of the latter isomer, and the peroxo/bis-($\mu$-oxo) equilibrium can be shifted from one extreme to the other within the same ligand system. Observations concerning the reactivity of the dioxygen adducts **2$^{H}$** and **3$^{NMe2}$** toward external substrates are also presented.

## Introduction

Ubiquitous copper ions in the active sites of proteins/enzymes mediate a broad scope of chemical processes including electron transfer, reversible dioxygen binding and activation, and nitrogen oxide transformations.[1−8] Biological binuclear copper centers involved with dioxygen binding and activation include hemocyanins (Hcs), tyrosinase (Tyr), and catechol oxidase (CO). Arthropodal and molluskan Hcs are blood $O_2$ carriers, Tyr is a widespread *o*-phenol hydroxylase, while CO converts catechols to quinones.[3−6] In these proteins, two copper(I) ions reduce $O_2$ to peroxide while generating a $\mu$-$\eta^2$:$\eta^2$-(side-on)-peroxo dicopper(II) structure (Figure 1).[9]

However, extensive biomimetic inorganic model studies have shown that Cu(I) can activate $O_2$ and bind ($O_2^{2-}$) in several different isoelectronic structural compositions.[4,5,10−12]

* Author to whom correspondence should be addressed. E-mail: karlin@jhu.edu.
† The Johns Hopkins University.
‡ Stanford University.

(1) *Bioinorganic Chemistry of Copper*; Karlin, K. D., Tyeklár, Z., Eds.; Chapman and Hall: New York, 1993.
(2) Klinman, J. P. *Chem. Rev.* **1996**, *96*, 2541−2561.
(3) Solomon, E. I.; Sundaram, U. M.; Machonkin, T. E. *Chem. Rev.* **1996**, *96*, 2563−2605.
(4) Lewis, E. A.; Tolman, W. B. *Chem. Rev.* **2004**, *104*, 1047−1076.
(5) Mirica, L. M.; Ottenwaelder, X.; Stack, T. D. P. *Chem. Rev.* **2004**, *104*, 1013−1045.
(6) Quant Hatcher, L.; Karlin, K. D. *JBIC, J. Biol. Inorg. Chem.* **2004**, *9*, 669−683.
(7) Wasser, I. M.; de Vries, S.; Moeenne-Loccoz, P.; Schroeder, I.; Karlin, K. D. *Chem. Rev.* **2002**, *102*, 1201−1234.
(8) Chen, P.; Gorelsky, S. I.; Ghosh, S.; Solomon, E. I. *Angew. Chem., Int. Ed.* **2004**, *43*, 4132−4140.
(9) Solomon, E. I.; Chen, P.; Metz, M.; Lee, S.-K.; Palmer, A. E. *Angew. Chem., Int. Ed.* **2001**, *40*, 4570−4590.
(10) Hatcher, L. Q.; Karlin, K. D. *J. Biol. Inorg. Chem.* **2004**, *9*, 669−683.
(11) Zhang, C. X.; Liang, H.-C.; Humphreys, K. J.; Karlin, K. D. In *Catalytic Activation of Dioxygen by Metal Complexes*; Simandi, L., Ed.; Kluwer: Dordrecht, The Netherlands, 2003; pp 79−121.
(12) Recently, a new $O_2$ binding mode having an $\eta^1$:$\eta^2$-$O_2$ structure has been characterized: Teramae, S.; Osako, T.; Nagatomo, S.; Kitagawa, T.; Fukuzumi, S.; Itoh, S. *J. Inorg. Biochem.* **2004**, *98*, 746.



10.1021/ic052185m CCC: $33.50 
Published on Web 03/02/2006

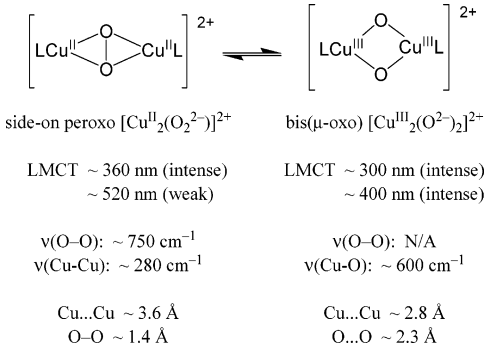


**Figure 1.** Equilibrium between side-on peroxo and bis($\mu$-oxo) dicopper cores and their foremost associated physical properties.

While nature selectively chooses the side-on peroxo binding mode (Figure 1), copper(I) complexes can also bind peroxide in a $\mu(1,2\text{-}O_2^{2-})$ "end-on" fashion to generate a $Cu^{II}_2(\mu\text{-}1,2\text{-}(O_2^{2-})$ species such as the well studied $[\{Cu^{II}(TMPA)\}_2(O_2^{2-})]$ (TMPA = tris(2-pyridyl)methylamine) complex.[13−18] Another feasible $Cu_2O_2$ structure is related to the $\mu\text{-}\eta^2\text{:}\eta^2$ side-on form but comprises a fully cleaved O−O bond producing a formal $Cu^{III}_2(\mu\text{-}O^{2-})_2$ species, first discovered by Tolman and co-workers and now well established in many different ligand systems (Figure 1).[5,6,19] Theoretical calculations predict that the free energies of dicopper(III) bis($\mu$-oxo) species are nearly identical to those of the side-on peroxo dicopper(II) isomer ($\Delta G° = 0.3-12.7$ kcal/mol), and the barrier for interconversion is very small.[20−24] Thermodynamic parameters were also experimentally obtained and demonstrate the energetic similarity: $\Delta H° = -0.6$ to $-3.8$ kcal/mol, and $\Delta S° = -2$ to $-20$ cal/mol·K.[25−27] Hence, with many ligand systems, $Cu_2O_2$ complexes coexist in a dynamic equilibrium between the dicopper(II) side-on peroxo and the dicopper(III) bis-$\mu$-oxo isomeric forms but which have now established distinctive spectroscopic and structural properties (Figure 1).[4,5,19,28] This equilibrium is especially intriguing to study because of the reversible O−O bond making/breaking process critical in dioxygen activation and oxidation chemistries employing $O_2$ or ROOH and the possible relevance to biological systems.

**Chart 1**

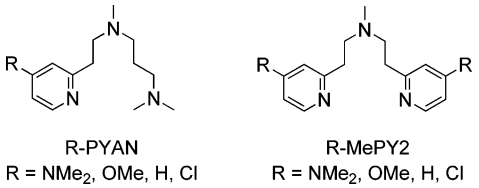


It has been well established that the coordinating ligand has a large effect on the resulting structure of the $2Cu^I/O_2$ adduct.[5,29] In general, tetradentate amine ligands tend to favor the formation of end-on peroxo dicopper(II) compounds,[13,18] while tridentate[30] and bidentate [31] ligands can generate both side-on peroxo and/or bis($\mu$-oxo) dicopper complexes.[32,33] Within the peroxo and bis($\mu$-oxo) realm, ligand denticity,[34] sterics,[26,35] and nitrogen donor type (alkyl vs pyridyl, or 2° vs 3° amine)[36,37] play important roles in the equilibrium between the isomeric $Cu_2O_2$ adducts.[38] To complicate matters further, changes in reaction conditions such as concentration,[39] temperature,[25] solvent,[27] or a change in counterion[26] can induce a shift in the equilibrium.[5]

With our own research program in copper−$O_2$ chemistry, we have also been interested in identifying and sorting out the principal features that dictate the resulting structure of $Cu_2O_2$ adducts. To these ends, we have synthesized a series of ligands that alter the electronic environment about the copper centers by adding electron-donating or electron-withdrawing groups to the para position of a pyridyl nitrogen donor. Previous studies on an analogous ligand system, R-MePY2 (bis[2-(4-R-2-pyridn-2-yl)ethyl]methylamine) (Chart 1), showed a marginal increase in bis($\mu$-oxo) formation

(13) Jacobson, R. R.; Tyeklár, Z.; Karlin, K. D.; Liu, S.; Zubieta, J. *J. Am. Chem. Soc.* **1988**, *110*, 3690−3692.
(14) Karlin, K. D.; Wei, N.; Jung, B.; Kaderli, S.; Zuberbühler, A. D. *J. Am. Chem. Soc.* **1991**, *113*, 5868−5870.
(15) Baldwin, M. J.; Ross, P. K.; Pate, J. E.; Tyeklár, Z.; Karlin, K. D.; Solomon, E. I. *J. Am. Chem. Soc.* **1991**, *113*, 8671−8679.
(16) Schatz, M.; Becker, M.; Thaler, F.; Hampel, F.; Schindler, S.; Jacobson, R. R.; Tyeklár, Z.; Murthy, N. N.; Ghosh, P.; Chen, Q.; Zubieta, J.; Karlin, K. D. *Inorg. Chem.* **2001**, *40*, 2312−2322.
(17) Zhang, C. X.; Kaderli, S.; Costas, M.; Kim, E.-i.; Neuhold, Y.-M.; Karlin, K. D.; Zuberbühler, A. D. *Inorg, Chem.* **2003**, *42*, 1807−1824.
(18) Komiyama, K.; Furutachi, H.; Nagatomo, S.; Hashimoto, A.; Hayashi, H.; Fujinami, S.; Suzuki, M.; Kitagawa, T. *Bull. Chem. Soc. Jpn.* **2004**, *77*, 59−72.
(19) Que, L., Jr.; Tolman, W. B. *Angew. Chem., Int. Ed.* **2002**, *41*, 1114−1137.
(20) Halfen, J. A.; Mahapatra, S.; Wilkinson, E. C.; Kaderli, S.; Young, V. G., Jr.; Que, L., Jr.; Zuberbühler, A. D.; Tolman, W. B. *Science* **1996**, *271*, 1397−1400.
(21) Cramer, C. J.; Smith, B. A.; Tolman, W. B. *J. Am. Chem. Soc.* **1996**, *118*, 11283−11287.
(22) Bérces, A. *Inorg, Chem.* **1997**, *36*, 4831−4837.
(23) Flock, M.; Pierloot, K. *J. Phys. Chem. A.* **1999**, *103*, 95−102.
(24) Henson, M. J.; Mukherjee, P.; Root, D. E.; Stack, T. D. P.; Solomon, E. I. *J. Am. Chem. Soc.* **1999**, *121*, 10332−10345.
(25) Cahoy, J.; Holland, P. L.; Tolman, W. B. *Inorg. Chem.* **1999**, *38*, 2161−2168.
(26) Mahadevan, V.; Henson, M. J.; Solomon, E. I.; Stack, T. D. P. *J. Am. Chem. Soc.* **2000**, *122*, 10249−10250.
(27) Liang, H.-C.; Henson, M. J.; Hatcher, L. Q.; Vance, M. A.; Zhang, C. X.; Lahti, D.; Kaderli, S.; Sommer, R. D.; Rheingold, A. L.; Zuberbuehler, A. D.; Solomon, E. I.; Karlin, K. D. *Inorg. Chem.* **2004**, *43*, 4115−4117.
(28) DuBois, J. L.; Mukherjee, P.; Stack, T. D. P.; Hedman, B.; Solomon, E. I.; Hodgson, K. O. *J. Am. Chem. Soc.* **2000**, *122*, 5775−5787.
(29) Mahadevan, V.; Klein Gebbink, R. J. M.; Stack, T. D. P. *Curr. Opin. Chem. Biol.* **2000**, *4*, 228−234.
(30) Lam, B. M. T.; Halfen, J. A.; Young, V. G., Jr.; Hagadorn, J. R.; Holland, P. L.; Lledos, A.; Cucurull-Sanchez, L.; Novoa, J. J.; Alvarez, S.; Tolman, W. B. *Inorg. Chem.* **2000**, *39*, 4059−4072.
(31) Cole, a. P.; Mahadevan, V.; Mirica, L. M.; Ottenwaelder, X.; Stack, T. D. P. *Inorg. Chem.* **2005**, *44*, 7345−7364.
(32) Osako, T.; Ohkubo, K.; Taki, M.; Tachi, Y.; Fukuzumi, S.; Itoh, S. *J. Am Chem. Soc.* **2003**, *125*, 11027−11033.
(33) Spencer, D. J. E.; Reynolds Anne, M.; Holland Patrick, L.; Jazdzewski, B. A.; Duboc-Toia, C.; Le Pape, L.; Yokota, S.; Tachi, Y.; Itoh, S.; Tolman William, B. *Inorg, Chem.* **2002**, *41*, 6307−6321.
(34) Teramae, S.; Osako, T.; Nagatomo, S.; Kitagawa, T.; Fukuzumi, S.; Itoh, S. *J. Inorg. Biochem.* **2004**, *98*, 746−757.
(35) Taki, M.; Teramae, S.; Nagatomo, S.; Tachi, Y.; Kitagawa, T.; Itoh, S.; Fukuzumi, S. *J. Am Chem. Soc.* **2002**, *124*, 6367−6377.
(36) Liang, H.-C.; Zhang, C. X.; Henson, M. J.; Sommer, R. D.; Hatwell, K. R.; Kaderli, S.; Zuberbuehler, A. D.; Rheingold, A. L.; Solomon, E. I.; Karlin, K. D. *J. Am Chem. Soc.* **2002**, *124*, 4170−4171.
(37) Mirica, L. M.; Vance, M.; Rudd, D. J.; Hedman, B.; Hodgson, K. O.; Solomon, E. I.; Stack, T. D. P. *J. Am Chem. Soc.* **2002**, *124*, 9332−9333.
(38) Stack, T. D. P. *Dalton Trans.* **2003**, 1881−1889.
(39) Mahapatra, S.; Kaderli, S.; Llobet, A.; Neuhold, Y.-M.; Palanché, T.; Halfen, J. A.; Young, V. G., Jr.; Kaden, T. A.; Que, L., Jr.; Zuberbühler, A. D.; Tolman, W. B. *Inorg. Chem.* **1997**, *36*, 6343−6356.

relative to side-on peroxo when adding electron-donating substituents, R = $NMe_2$ and OMe, compared to R = H.[40] However, the $Cu_2O_2$ adducts were always a mixture of both $Cu^{II}{}_2(O_2)$ and $Cu^{III}{}_2(O)_2$ in equilibrium, and the peroxide O−O bond strength remained unaffected.[41] We also previously reported on the copper(I) complex of H-PYAN (*N*-[2-(pyridin-2-yl)ethyl]-*N*,*N*′,*N*′-trimethyl-propane-1,3-diamine) (Chart 1) which reacts with $O_2$ to generate a mixture of side-on peroxo and bis($\mu$-oxo) dicopper compounds, with the equilibrium being highly solvent dependent.[27] In THF, the resulting dioxygen adduct was roughly a 50/50 mixture of side-on peroxo dicopper(II) and bis($\mu$-oxo) dicopper(III), providing a unique system to study ligand electronic effects on that midway equilibrium. The ligands, R-PYAN (*N*-[2-(4-R-pyridin-2-yl)-ethyl]-*N*,*N*′,*N*′-trimethyl-propane-1,3-diamine) where R = $NMe_2$, OMe, H, and Cl, have now been synthesized in order to isolate and study solely the electronic effects on the peroxo/oxo equilibrium without altering any other aspects (e.g., sterics, denticity, solvent, etc.). The copper(I) complexes of R-PYAN have been studied with respect to redox potential, CO binding, and dioxygen reactivity. UV−visible and resonance Raman (rR) spectroscopy have been employed to determine the ligand-electronic effects on the $\mu$-$\eta^2$:$\eta^2$-(side-on)-peroxo dicopper(II) and bis-$\mu$-oxo dicopper(III) equilibrium. To compare and contrast, the ligand system R-MePY2 (Chart 1) and its $Cu^I/O_2$ reactivity are also discussed.

## Experimental Section

**General Considerations and Instrumentation.** Elemental analyses were performed by Desert Analytics, Tucson, AZ. Mass spectrometry was conducted at the mass spectrometry (MS) facility at either the Johns Hopkins University or at the Ohio State University. CI spectra were acquired at the Johns Hopkins University MS facility using a VG70S double-focusing magnetic sector mass spectrometer (VG Analytical, Manchester, UK, now Micromass/Waters) equipped with a Xe gas FAB gun (7.5 kV at 1 mA) and an off-axis electron multiplier. Samples were introduced into the CI source (block temperature = 200 °C) using a heated direct insertion probe using a deep quartz cup at a rate of 0.5 °C/s. Methane reagent gas was used with an electron energy of 70 eV. High-boiling perfluorokerosene was used as the reference mass for accurate mass analyses. For accurate mass analyses, the matrix contained 10% PEG mass calibrant. Data were acquired using a MSS Data system (MasCom, Bremen, Germany) for subsequent processing. High-resolution electrospray ionization (ESI) mass spectrometry analyses were performed at the Ohio State University (MS) facility with a 3-T Finnigan FTMS-2000 Fourier transform mass spectrometer. Samples were sprayed from a commercial Analytical electrospray ionization source, and then focused into the FTMS cell using a home-built set of ion optics. X-ray diffraction was performed at the X-ray diffraction facility at the Johns Hopkins University with an Xcalibur3 diffractometer.[42] $^1$H NMR and $^{13}$C NMR spectra were measured on a Varian 400 MHz spectrometer, chemical shifts are reported in ppm downfield from an internal TMS reference, and *J* values are reported in hertz. Infrared spectra were recorded on a Bruker vector 22 infrared spectrometer.

Low-temperature UV−vis spectra were taken either with a Hewlett-Packard model 8453 diode array spectrophotometer equipped with a custom-made quartz Dewar filled with cold (−78 °C) methanol (maintained and controlled by a Neslab ULT-95 low-temperature recirculating unit), or using a −78 °C methanol bath (maintained by a CC-100 immersion cooler and Agitainor, Neslab) and taking measurements with a Cary 50 Bio spectrophotometer equipped with a fiber optic coupler (Varian) and a fiber optic dip probe (Hellma 661.302-QX-UV, 2 mm for low temperature). Air-sensitive solutions were prepared in a nitrogen atmosphere in a glovebox (MBraun) and carried out in 2 mm Schlenk cuvettes (Quark) or custom-made Schlenk tubes designed for the fiber-optic dip probe (Chemglass, part no. JHU-0407-271-MS).

Resonance Raman (rR) spectroscopy was performed with a Princeton Instruments ST-135 back-illuminated CCD detector on a Spex 1877 CP triple monochromator with 1200, 1800, and 2400 grooves/mm holographic spectrograph gratings. Excitation was provided by a Coherent I90C-K Kr+ ion laser. The spectral resolution was $<2$ cm$^{-1}$. Sample concentrations were ~1 mM in $Cu_2O_2$. For resonance enhancement at 364 and 407 nm, samples were run at 77 K in a liquid $N_2$ finger Dewar (Wilmad) and were hand-spun to minimize sample decomposition during scan collection. To observe the peroxide stretching frequency, excitation was at 531 nm and samples were run at 193 K. Isotopic substitution was achieved by oxygenating with $^{18}O_2$ (Icon, Summit, NJ).

Cyclic voltammetry measurements were undertaken in freshly distilled dimethylformamide (DMF) with a BAS 100B electrochemical analyzer with a glassy carbon working electrode and a platinum wire auxiliary electrode. Potentials were recorded versus a saturated calomel reference electrode. $E_{1/2}$ values are reported versus the $Fe(cp)_2^{+/0}$ couple according to $Fe(cp)_2^{+/0} = 0.45$ V vs SCE in DMF with $[Bu_4N][PF_6]$.[43] Scans were run at 50−300 mV/s under an argon atmosphere using ca. 0.1 M $[Bu_4N][PF_6]$ as the supporting electrolyte.

GC analyses were carried out on a HP-5890 Series II gas chromatograph using an Rtx-5 (crossbonded 5% diphenyl 95% dimethyl polysiloxane) 30 m × 0.32 mm I.D. × 0.25 $\mu$m film thickness and analyzed with a flame ionization detector connected to peak simple chromatography data system from SRI. GC conditions. Benzyl alcohol: inject/detector temp, 250 °C; oven temp, 110 °C; column head pressure, 115 kPa; purge vent, 5 mL/min; split vent, 55 mL/min; total flow, 65 mL/min. Dihydroanthracene: inject/detector temp, 350 °C; oven temp, 120 °C for 2 min then ramped at 30 °C/min until temperature reached 210 °C; column head pressure, 120 kPa; purge vent, 5 mL/min; split vent, 55 mL/min; total flow 61 mL/min. Dimethylaniline: inject/detector temp, 250 °C; oven temp, 100 °C; column head pressure, 120 kPa; purge vent, 5 mL/min; split vent, 55 mL/min; total flow, 67 mL/min. Thioanisole: inject/detector temp, 250 °C; oven temp, 120 °C for 2 min then ramped at 15 °C/min until temperature reached 145 °C; column head pressure, 120 kPa; purge vent, 5 mL/min; split vent, 55 mL/min; total flow, 67 mL/min.

**Synthesis of Ligands and Copper Complexes.** Reagents and solvents used were of commercially available reagent quality unless otherwise stated. Methylene chloride was purified by being passed

(40) Zhang, C. X.; Liang, H.-C.; Kim, E.-i.; Shearer, J.; Helton, M. E.; Kim, E.; Kaderli, S.; Incarvito, C. D.; Zuberbühler, A. D.; Rheingold, A. L.; Karlin, K. D. *J. Am Chem. Soc.* **2003**, *125*, 634−635.

(41) Henson, M., J.; Vance, M. A.; Zhang, C. X.; Liang, H.-C.; Karlin, K. D.; Solomon, E. I. *J. Am Chem. Soc.* **2003**, *125*, 5186−5192.

(42) Crystals suitable for diffraction were obtained by layering pentane over a saturated $CH_2Cl_2$ solution of $\mathbf{1}^{\mathbf{Cl}}$ kept under argon and by dissolving $\mathbf{1}^{\mathbf{NMe2}}$ into a mixture of $CH_3NO_2$/THF/$Et_2O$ and then layered with pentane. Residual $O_2$ in the glovebox oxidized the complex, and crystals of $\mathbf{4}^{\mathbf{NMe2}}$ were obtained.

(43) Connelly, N. G.; Geiger, W. E. *Chem. Rev.* **1996**, *96*, 877−910.

through a double alumina column solvent purification system by Innovative Technologies, Inc. Tetrahydrofuran was purified by distillation from sodium/benzophenone under argon. Acetone was distilled from Drierite under argon. HPLC grade pentane was purchased from Fisher Scientific. Air-sensitive compounds were synthesized and handled under an argon atmosphere using standard Schlenk techniques and stored in an MBraun drybox filled with $N_2$. Deoxygenation of solvents was achieved either by bubbling argon through the solution for 30−45 min or by applying three freeze−pump−thaw cycles. 4-R-2-vinylpyridine (R = $NMe_2$, OMe, Cl),[40] H−PYAN,[27] $[Cu(MeCN)_4][B(C_6F_5)_4]$[44] and $[Cu(H-PYAN)(MeCN)]B(C_6F_5)_4$[27] were synthesized as previously reported.

***N*-[2-(4-(Dimethylamino)-pyridin-2-yl)-ethyl]-*N,N′,N′*-trimethyl-propane-1,3-diamine ($NMe_2$-PYAN).** In a 50-mL round-bottom flask, *N,N,N′*-trimethyl-1,3-propanediamine (0.964 g, 0.0083 mol) and 4-(dimethylamino)-2-vinylpyridine (1.23 g, 0.0083 mol) were added along with 5 mL of MeOH and a few drops of glacial acetic acid. The reaction mixture was refluxed for 3 days at 100 °C. The crude reaction mixture was collected after rotary evaporation and purified by column chromatography using 2% MeOH/EtOAc on alumina to give 0.920 g (42% yield) of the pure oil. ($R_f$ = 0.2 in 2% MeOH/EtOAc on alumina, or 0.2 in 98% MeOH/2% $NH_4OH$ on silica). $^1$H NMR ($CDCl_3$): $\delta$ 8.13 (1 H, py-6, d ($J$ = 2.8)), 6.37 (1 H, py-3, d ($J$ = 1.2)), 6.33 (1 H, py-5, dd($J$ = 3)), 2.97 (6 H, s), 2.81 (2 H, m), 2.76 (2 H, m), 2.43 (2 H, t ($J$ = 3.8)), 2.30 (3 H, s), 2.25 (2 H, t ($J$ = 3.6)), 2.19 (6 H, s), 1.65 (2H, quint ($J$ = 3.8)). $^{13}$C NMR ($CDCl_3$): $\delta$ 160.6, 154.9, 149.4, 105.7, 104.7, 58.1, 58.0, 55.8, 45.7, 42.4, 39.6, 34.3, 25.9. EI-MS $m/z$ = 265.2 (M + $H^+$).

***N*-[2-(4-Methoxy-pyridin-2-yl)-ethyl]-*N,N′,N′*-trimethyl-propane-1,3-diamine (OMe-PYAN).** In a 50-mL round-bottom flask, *N,N,N′*-trimethyl-1,3-propanediamine (153 mg, 0.00132 mol) and a slight excess of 4-methoxy-2-vinylpyridine (200 mg, 0.00148 mol) were added along with 5 mL of MeOH and a few drops of glacial acetic acid. The reaction mixture was refluxed for 3 days at 70−90 °C. The crude reaction mixture was rotary evaporated and purified by column chromatography using 3% MeOH/EtOAc on alumina to give 155 mg (46% yield) of the pure oil. ($R_f$ = 0.2 in 3% MeOH/EtOAc on alumina, or 0.25 in 98% MeOH/2% $NH_4OH$ on silica). $^1$H NMR ($CDCl_3$): $\delta$ 8.32 (1 H, py-6, d ($J$ = 3)), 6.69 (1 H, py-3, d ($J$ = 1.2)), 6.64 (1 H, py-5, dd ($J$ = 3, 1.2)), 3.82 (3 H, s), 2.86 (2 H, m), 2.75 (2 H, m), 2.42 (2 H, t ($J$ = 3.8)), 2.30 (3 H, s), 2.24 (2 H, t ($J$ = 3.6)), 2.195 (6 H, s), 1.64 (2H, quint ($J$ = 3.8)). $^{13}$C NMR ($CDCl_3$): $\delta$ 166.1, 162.4, 150.6, 109.2, 107.6, 58.1, 57.6, 55.8, 55.2, 45.7, 42.3, 36.2, 25.8. EI-MS $m/z$ = 252.2 (M + $H^+$).

***N*-[2-(4-Chloro-pyridin-2-yl)-ethyl]-*N,N′,N′*-trimethyl-propane-1,3-diamine (Cl-PYAN):** In a 50-mL round-bottom flask, *N,N,N′*-trimethyl-1,3-propanediamine (250 mg, 0.00215 mol) and a slight excess of 4-chloro-2-vinylpyridine (322 mg, 0.00231 mol) were added along with 5 mL of MeOH and a few drops of glacial acetic acid. The reaction mixture was refluxed for 3 days at 70−90 °C. The crude reaction mixture was rotavapped and purified by column chromatography using 3% MeOH/EtOAc on alumina to give 245 mg (44% yield) of the pure oil. ($R_f$ = 0.5−0.3, 3% MeOH/EtOAc on alumina, or 0.3−0.2 in 98% MeOH/2% $NH_4OH$ on silica). $^1$H NMR ($CDCl_3$): $\delta$ 8.41 (1 H, py-6, d ($J$ = 2.8)), 7.21 (1 H, py-3, d ($J$ = 1)), 7.13 (1 H, py-5, dd ($J$ = 2.8, 1)), 2.92 (2 H, m), 2.76 (2 H, m), 2.43 (2 H, t ($J$ = 3.8)), 2.24 (3 H, s), 2.24 (2 H, t ($J$ = 3.6)), 2.205 (6 H, s), 1.63 (2H, quint ($J$ = 3.6)). $^{13}$C NMR ($CDCl_3$): $\delta$ 166.1, 162.4, 150.6, 109.2, 107.6, 58.1, 57.6, 55.8, 55.2, 45.7, 42.3, 36.2, 25.8. High-resolution ESI-MS Calcd (M + $H^+$): $m/z$ = 256.15750, Found: $m/z$ = 256.15659.

**Synthesis of $[Cu(NMe_2\text{-PYAN})][B(C_6F_5)_4]$.** Under an Ar atmosphere using air-free glassware, a solution of $NMe_2$-PYAN (190 mg, 7.16 × $10^{-4}$ mol) in 6 mL of deoxygenated $CH_2Cl_2$ was added to solid $[Cu(MeCN)_4][B(C_6F_5)_4]$ (645 mg, 7.11 × $10^{-4}$ mol). The resulting peachy-pink solution was allowed to stir for 30 min at room temperature and then was gravity filtered through a medium-porosity frit under argon. The small amount of orange solid collected was unreactive toward $O_2$ and discarded. To the pink filtrate was added deoxygenated pentane (∼80 mL) and left to stand at −78 °C under argon for 2 h, after which an oil separated. The supernatant solution was removed by cannula, and the oil was dried in vacuo to yield 537 mg (75%) of light pink powder. Anal. Calcd for ($C_{39}H_{28}BCuF_{20}N_4$): C, 46.52; H, 2.80; N, 5.56. Found: C, 46.31; H, 2.41; N, 5.79.

**Synthesis of $[Cu(OMe\text{-}PYAN)(MeCN)][B(C_6F_5)_4]$.** Under an argon atmosphere using air-free glassware, a solution of OMe-PYAN (125 mg, 4.97 × $10^{-4}$ mol) in 8 mL of deoxygenated $CH_2Cl_2$ was added to solid $[Cu(MeCN)_4][B(C_6F_5)_4]$ (645 mg, 7.11 × $10^{-4}$ mol). The resulting olive-colored solution was allowed to stir for 30 min at room temperature and then gravity filtered through a medium-porosity frit under argon. The small amount of orange solid was unreactive toward $O_2$ and discarded. To the dark yellow filtrate was added deoxygenated pentane (∼80 mL) and left to stand at −78 °C under argon for 2 h, after which oil separated. The colorless supernatant solution was removed by cannula, and the oil was dried in vacuo to yield 411 mg (78%) of light green powder. Anal. Calcd for ($C_{40}H_{28}BCuF_{20}N_4O$): C, 46.42; H, 2.73; N, 5.41. Found: C, 47.04; H, 2.68; N, 5.36.

**Synthesis of $[Cu(Cl\text{-}PYAN)(MeCN)][B(C_6F_5)_4]$.** Under an argon atmosphere using air-free glassware, a solution of Cl-PYAN (6.7 mg, 2.62 × $10^{-4}$ mol) in ∼10 mL of deoxygenated $CH_2Cl_2$ was added to solid $[Cu(MeCN)_4][B(C_6F_5)_4]$ (237 mg, 2.61$^{-4}$ mol). The resulting clear, bright, yellow solution was allowed to stir for 30 min at room temperature, and then deoxygenated pentane (∼70 mL) was added with stirring at −78 °C under argon until a precipitate formed. The reaction mixture was filtered under argon through a coarse-porosity frit, and the solid was dried in vacuo to yield 233 mg (82%) light yellow solid. Anal. Calcd for ($C_{39}H_{25}BClCuF_{20}N_4$): C, 45.07; H, 2.42; N, 5.39. Found: C, 45.54; H, 2.47; N, 5.24.

**Synthesis of $[Cu(R\text{-}PYAN)(CO)]B(C_6F_5)_4$ Complexes.** CO adducts were generated in situ by bubbling CO through an air-free $CH_2Cl_2$ solution of the corresponding Cu(I) complex.

**Synthesis of $[\{Cu(R\text{-}PYAN)\}_2(OH)_2][B(C_6F_5)_4]_2$ Complexes.** The dicopper(II) dihydroxy compounds were prepared by adding $O_2$ to a $CH_2Cl_2$ solution of $[Cu(R\text{-}PYAN)(MeCN)_n]B(C_6F_5)_4$ at −78 °C and left at −80 °C overnight. The solutions were then warmed to room temperature, and the copper(II) decomposition product was precipitated by the addition of pentane. Anal. Calcd for $[\{Cu(NMe_2\text{-}PYAN)\}_2(OH)_2][B(C_6F_5)_4]_2\cdot CH_2Cl_2\cdot C_5H_{12}$ ($C_{84}H_{72}B_2Cl_2Cu_2F_{40}N_8O_2$): C, 45.75; H, 3.29; N, 5.08. Found: C, 45.35; H, 3.20; N, 5.00. Anal. Calcd for $[\{Cu(OMe\text{-}PYAN)\}_2(OH)_2][B(C_6F_5)_4]_2\cdot CH_2Cl_2\cdot C_5H_{12}$ ($C_{82}H_{66}B_2Cl_2Cu_2F_{40}N_6O_4$): C, 45.20; H, 3.05; N, 3.86. Found: C, 44.78; H, 2.43; N, 3.58. Anal. Calcd for $[\{Cu(H\text{-}PYAN)\}_2(OH)_2][B(C_6F_5)_4]_2\cdot CH_2Cl_2\cdot C_5H_{12}$ ($C_{80}H_{62}B_2Cl_2Cu_2F_{40}N_6O_2$): C, 45.35; H, 2.95; N, 3.97. Found: C, 45.57; H, 3.20; N, 4.18. Anal. Calcd for $[\{Cu(Cl\text{-}PYAN)\}_2(OH)_2][B(C_6F_5)_4]_2\cdot C_5H_{12}$ ($C_{79}H_{58}B_2Cl_2Cu_2F_{40}N_6O_2$): C, 45.12; H, 2.78; N, 4.00. Found: C, 45.43; H, 3.34; N, 4.08.

**Exogenous Substrate Oxidations.** The general procedure for substrate oxidations is as follows. The Cu(I) solutions (2 mL, ∼(3−

(44) Liang, H.-C.; Kim, E.; Incarvito, C. D.; Rheingold, A. L.; Karlin, K. D. *Inorg. Chem.* **2002**, *41*, 2209−2212.

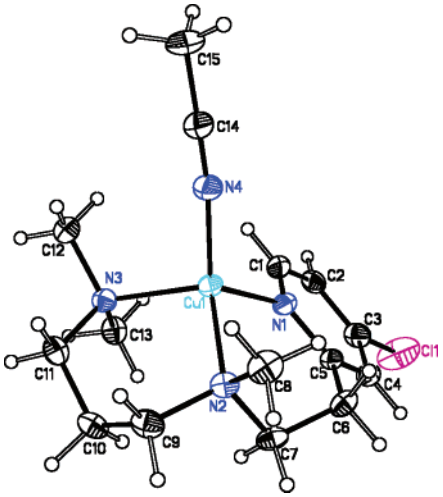


**Figure 2.** ORTEP diagram (at 50% probability) of the cationic portion $[Cu^{I}(Cl\text{-}PYAN)(MeCN)]B(C_6F_5)_4$ ($\mathbf{1^{Cl}}$).

4) × $10^{-5}$ M) were prepared in the drybox and then brought out and handled in Schlenk tubes. The solutions were cooled to −78 °C with an acetone/dry ice bath. Dry $O_2$ gas was bubbled through the solutions for a few minutes, and enough time was allowed to generate full formation of the peroxo or oxo adduct. Excess $O_2$ was then purged by three vacuum/Ar purge cycles and bubbling argon through the solutions for at least 60 s. Then, 1 equiv of the internal standard (decane) and 10 equiv of substrate were added in $CH_2Cl_2$ solutions. Argon was bubbled again to remove any dissolved $O_2$ in the substrate/internal standard, and the reaction was allowed to proceed under argon for 20−24 h. Finally, pentane was added to the green solutions to precipitate the copper complex and analyze the supernatant organic substrates by GC. Yields reported are an average of five or six runs.

## Results and Discussion

**Synthesis and Physical Properties of $\mathbf{1^R}$.** The new ligands R-PYAN (*N*-[2-(4-R-pyridin-2-yl)-ethyl]-*N*,*N*′,*N*′-trimethyl-propane-1,3-diamine, where R = $NMe_2$, OMe, and Cl) were synthesized and characterized by $^1H$ and $^{13}C$ NMR spectroscopy and mass spectrometry. The corresponding copper(I) complexes were synthesized by the anaerobic addition of the ligand to $[Cu^{I}(CH_3CN)_4]B(C_6F_5)_4$ dissolved in dichloromethane. Upon isolation (see Experimental Section), the $[Cu^{I}(R\text{-}PYAN)(CH_3CN)_n]B(C_6F_5)_4$ complexes ($\mathbf{1^R}$) ($n$ = 1 for R = Cl, H, and OMe; $n$ = 0 for R = $NMe_2$) were characterized by elemental analysis, and $[Cu(Cl\text{-}PYAN)(MeCN)]B(C_6F_5)_4$ ($\mathbf{1^{Cl}}$) was recrystallized to yield crystals suitable for X-ray diffraction.

The structure of the cationic portion of $\mathbf{1^{Cl}}$ is shown in Figure 2 and depicts a distorted tetrahedral copper center, with three N donors from the PYAN ligand and a fourth N donor from acetonitrile, similar to other Cu(I) complexes of tridentate pyridylalkylamine ligands including $[Cu(H\text{-}PYAN)(MeCN)]B(C_6F_5)_4$ ($\mathbf{1^H}$).[27] $[Cu(OMe\text{-}PYAN)(MeCN)]B(C_6F_5)_4$ ($\mathbf{1^{OMe}}$) also binds acetonitrile, while the complex with the most electron donating ligand $[Cu(NMe_2\text{-}PYAN)]B(C_6F_5)_4$ ($\mathbf{1^{NMe2}}$) is stable as a tridentate and does not seem to require an additional nitrogen donor; unlike the others, it is readily isolated without a strong MeCN ligand, even in the presence of MeCN in solution.

**Table 1.** Selected Bond Angles and Distances for $[Cu(Cl\text{-}PYAN)(MeCN)]B(C_6F_5)_4$ ($\mathbf{1^{Cl}}$) and $[Cu(H\text{-}PYAN)(MeCN)]B(C_6F_5)_4$ ($\mathbf{1^H}$)

| angle[a] (deg) | $1^{Cl}$ | $\mathbf{1^H}$ [b] |
|---|---|---|
| ∠N(1)−Cu(1)−N(3) | 107.62 (6) | 109.77 (6) |
| ∠N(1)−Cu(1)−N(2) | 101.00 (6) | 101.56 (7) |
| ∠N(2)−Cu(1)−N(3) | 103.45 (6) | 102.20 (6) |
| ∠N(1)−Cu(1)−N(4) | 119.91 (7) | 119.87 (7) |
| ∠N(2)−Cu(1)−N(4) | 117.18 (7) | 117.18 (7) |
| ∠N(3)−Cu(1)−N(4) | 106.29 (6) | 104.90 (7) |
| **distance (Å)** | **$1^{Cl}$** | **$\mathbf{1^H}$ [b]** |
| Cu(1)−N(1) | 2.0297 (15) | 2.0399 (17) |
| Cu(1)−N(2) | 2.0997 (15) | 2.1145 (17) |
| Cu(1)−N(3) | 2.1405 (16) | 2.1527 (16) |
| Cu(1)−N(4) | 1.9268 (17) | 1.9437 (18) |

[a] According to atom labels depicted in Figure 2. [b] From ref 27.

**Table 2.** Copper(I) Complex Reduction Potentials and Carbonyl Stretching Frequencies

| $E_{1/2}$[a] vs $Fe(cp)_2^{+/0}$ (V)[b] | | $\nu$(C−O) ($cm^{-1}$) | |
|---|---|---|---|
| $\mathbf{1^{NMe2}}$ | −0.40 | $\mathbf{1^{NMe2}}$**−CO** | 2080 |
| $\mathbf{1^{OMe}}$ | −0.38 | $\mathbf{1^{OMe}}$**−CO** | 2086 |
| $\mathbf{1^H}$ | −0.33 | $\mathbf{1^H}$**−CO** | 2088 |
| $\mathbf{1^{Cl}}$ | −0.32 | $\mathbf{1^{Cl}}$**−CO** | 2090 |

[a] In *N*,*N*-dimethylformamide. [b] According to $Fe(cp)_2^{+/0}$ = 0.45 V vs SCE.[45]

The copper(I) complex $\mathbf{1^{Cl}}$ has remarkable structural resemblance to that of the parent compound $\mathbf{1^H}$. A comparison of the structural parameters for $\mathbf{1^{Cl}}$ and $\mathbf{1^H}$ is listed in Table 1. The virtually superimposable geometry (along with both bond distances and angles) around the copper(I) ion is a clear indication that the ligand modification by the 4-R-pyridyl substituent does not affect the steric environment around the copper center. Although the exact ligand geometry of the $Cu^{II}_2O_2$ adducts is unknown, the similarities of the crystal structures of $\mathbf{1^{Cl}}$ and $\mathbf{1^H}$ suggest that the R-PYAN ligand series will dominantly induce an electronic effect in its $Cu^{I}/O_2$ reactivity.

**Electrochemistry.** The redox potentials of the $Cu^{II}/Cu^{I}$ couple for the complexes was determined by cyclic voltammetry in DMF solvent (Supporting Information) to assess the electronic influence induced by the 4-R-pyridyl substituent. The $E_{1/2}$ values for $\mathbf{1^{NMe2}}$, $\mathbf{1^{OMe}}$, $\mathbf{1^H}$, and $\mathbf{1^{Cl}}$ are −0.40, −0.38, −0.33, and −0.32 V vs $Fe(cp)_2^{+/0}$ in DMF,[45] respectively (Table 2), indicating that, as expected, the more electron rich copper(I) complexes with better R-donors are easier to oxidize than those with electron-deficient substituents. These values are similar to those of the complexes containing the ligand series R-MePY2, where the $E_{1/2}$ values are −0.44, −0.36, −0.31, and −0.27 V vs $Fe(cp)_2^{+/0}$ in DMF for R = $NMe_2$, OMe, H, and Cl, respectively.[40] However, the overall range of redox potentials of 0.08 V for the series $\mathbf{1^R}$ is considerably less than that of 0.17 V observed for the $Cu^{II}/Cu^{I}$ couple for the ligands R-MePY2. This result is perhaps expected, since the ligand system R-MePY2 has double the substituent effects versus R-PYAN; the former ligand contains two pyridyl nitrogen ($N_{py}$) donors versus the one $N_{py}$ donor in R-PYAN (Chart 1).

(45) Converted value according to $Fc^{+/0}$ $E_{1/2}$ = 0.45 V vs SCE in DMF (Connelly, N. G, Geiger, W. E. *Chem. Rev.* **1996**, *96*, 877−910).

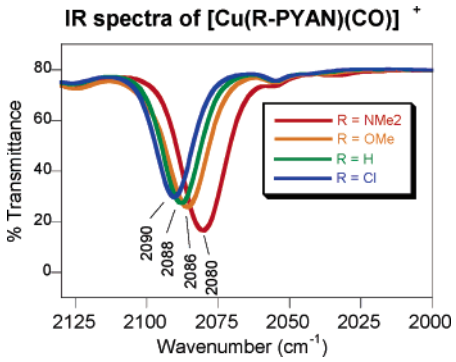


**Figure 3.** Solution ($CH_2Cl_2$) C−O stretching frequencies of $\mathbf{1^R}$ **−CO**.

**Carbon Monoxide Adducts.** The study of carbon monoxide binding to metal centers is a useful approach to probe bonding and structure, as well as having been used to stabilize reactive copper(I) complexes for X-ray crystallographic analysis.[46] The diatomic CO molecule is also often used as a surrogate for $O_2$-binding studies. It is also common to use CO to probe the relative amount of back-bonding a given metal complex bestows on the bound CO; the more electron-rich a metal center, the more back-bonding occurs, and this is manifested by a lowered carbonyl stretching frequency. For this latter purpose, the carbonyl adducts $\mathbf{1^R}$**-CO** were synthesized in situ by bubbling CO(g) through a methylene chloride solution of $\mathbf{1^R}$ and solution IR spectra were recorded (Figure 3). As expected, the complex with the most electron donating ligand, $\mathbf{1^{NMe2}}$**-CO**, possesses the lowest carbonyl stretching frequency, 2080 $cm^{-1}$. The next most electron donating copper(I) complex, $\mathbf{1^{OMe}}$**-CO,** has a slightly stronger carbon monoxide bond with $\nu$(C−O) = 2086 $cm^{-1}$. The parent and chloro-substituted analogues do not differ much from $\mathbf{1^{OMe}}$**-CO** as $\nu$(C−O) = 2088 and 2090 $cm^{-1}$ for $\mathbf{1^H}$**-CO** and $\mathbf{1^{Cl}}$**-CO**, respectively. Thus, the substituted ligands impose only a minor change in the ligand−$Cu^I$−CO carbonyl stretching frequency, suggesting that the difference in back-bonding as a result of the varying R substituent is quite small, although measurable. The CO stretching frequencies are similar to those reported for [Cu(R-MePY2)(CO)]$^+$ where $\nu$(C−O) ranges from 2075 to 2093 $cm^{-1}$; however, notice the range in values is again larger in this latter case.[40] As described above, this is probably a result of the R-MePY2 ligand system having essentially two times the substituent effect than the R-PYAN system.

**Dioxygen Reactivity of [Cu(R-PYAN)(MeCN)$_n$]B(C$_6$F$_5$)$_4$ ($\mathbf{1^R}$).** According to the physical structures, redox potentials, and $\nu$(C−O) of $[LCu^I(CO)]^+$ of $\mathbf{1^R}$ and in comparison to the copper(I) complexes of R-MePY2, one might think the dioxygen reactivity would follow a very similar pattern. Indeed, both sets of copper(I) complexes react with dioxygen as outlined in Scheme 1, where the low-temperature stable dioxygen adducts, $\mathbf{2^R}$ and $\mathbf{3^R}$, can be in equilibrium; upon warming, these transform to the more stable dihydroxy-bridged dicopper(II) complexes, $\mathbf{4^R}$ (vide infra).

**Scheme 1**

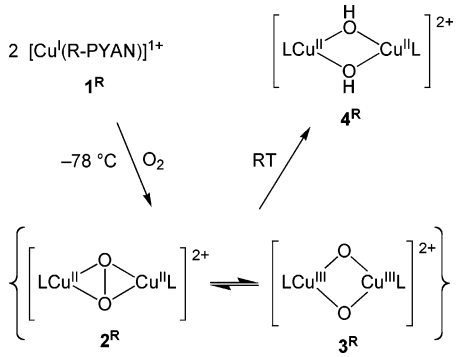


As examined by low-temperature UV−vis spectroscopy, the dioxygen reactivity with $\mathbf{1^R}$ is considerably different than that of the $Cu^I$ complexes of R-MePY2, whereby the R substituent in R-PYAN induces a substantial effect on the resulting dioxygen intermediate. For example, in THF at −78 °C, $\mathbf{1^H}$ reacts with $O_2$ forming an approximately equal mixture of side-on peroxo $[\{Cu^{II}(H\text{-}PYAN)\}_2(O_2)]^{2+}$ ($\mathbf{2^H}$) and bis($\mu$-oxo) $[\{Cu^{III}(H\text{-}PYAN)\}_2(O)_2]^{2+}$ ($\mathbf{3^H}$) adducts according to the intensities of the LMCT band at 360 nm corresponding to $\mathbf{2^H}$ and the one at 395 nm corresponding to $\mathbf{3^H}$—assuming that the $\epsilon$ values for the pure side-on peroxo and bis($\mu$-oxo) dicopper complexes fall within the range for previously reported systems (Scheme 1 and Figure 4).[24,27,35,47−49] However, the copper(I) complex containing an electron-withdrawing ligand substituent, $\mathbf{1^{Cl}}$, reacts with $O_2$ to form predominantly the side-on peroxo adduct, $[\{Cu^{II}(Cl-PYAN)\}_2(O_2)]^{2+}$ ($\mathbf{2^{Cl}}$) with the bis($\mu$-oxo) isomer, $[\{Cu^{III}(Cl-PYAN)\}_2(O)_2]^{2+}$ ($\mathbf{3^{Cl}}$), being a minor product (Figure 4, top). On the other hand, the complex with the electron-donating methoxy substituent, $\mathbf{1^{OMe}}$, preferentially binds $O_2$ in a bis($\mu$-oxo) dicopper(III) structure, $[\{Cu^{III}(OMe\text{-}PYAN)\}_2(O)_2]^{2+}$ ($\mathbf{3^{OMe}}$), with very little side-on peroxo $[\{Cu^{II}(OMe\text{-}PYAN)\}_2(O_2)]^{2+}$ ($\mathbf{2^{OMe}}$) in equilibrium. Finally, on the basis of these UV−vis spectroscopic interrogations, $\mathbf{1^{NMe2}}$ favors exclusively the bis($\mu$-oxo) $[\{Cu^{III}(NMe_2-PYAN)\}_2(O)_2]^{2+}$ ($\mathbf{3^{NMe2}}$) adduct (Figure 4, top). Hence, the one pyridyl substituent on R-PYAN imposes a dramatic electronic (due to substituent) effect on dioxygen reactivity such that the equilibrium between the dioxygen isomers is shifted from mostly a side-on peroxo species $\mathbf{2^{Cl}}$ to a bis($\mu$-oxo) structure $\mathbf{3^{NMe}}$ (Figure 5).

The effect of solvent is known to be a factor in the equilibrium between the isomeric side-on peroxo and bis($\mu$-oxo) dicopper cores, whereby coordinating solvents bias the equilibrium toward the bis($\mu$-oxo) structure.[25−27] To catalog the solvent effects on the dioxygen reactivity of [Cu(R-PYAN)(MeCN)$_n$]B(C$_6$F$_5$)$_4$ ($\mathbf{1^R}$), oxygenation reactions were also carried out in methylene chloride (Figure 4,

(46) Karlin, K. D.; Tyeklár, Z.; Farooq, A.; Haka, M. S.; Ghosh, P.; Cruse, R. W.; Gultneh, Y.; Hayes, J. C.; Toscano, P. J.; Zubieta, J. *Inorg. Chem.* **1992**, *31*, 1436−1451.

(47) Mahapatra, S.; Halfen, J. A.; Wilkinson, E. C.; Pan, G.; Wang, X.; Young, J., V. G.; Cramer, C. J.; Que, J., L.; Tolman, W. B. *J. Am. Chem. Soc.* **1996**, *118*, 11555−11574.

(48) Mahadevan, V.; DuBois, J. L.; Hedman, B.; Hodgson, K. O.; Stack, T. D. P. *J. Am. Chem. Soc.* **1999**, *121*, 5583−5584.

(49) According to the calculated spectra derived from kinetics analyses, the $\epsilon$ values for pure $\mathbf{2^H}$ and $\mathbf{3^H}$ are 21 000 ($\lambda_{max}$ = 360) and 25 000 $M^{-1}$ $cm^{-1}$ ($\lambda_{max}$ = 400), respectively. See ref 29.

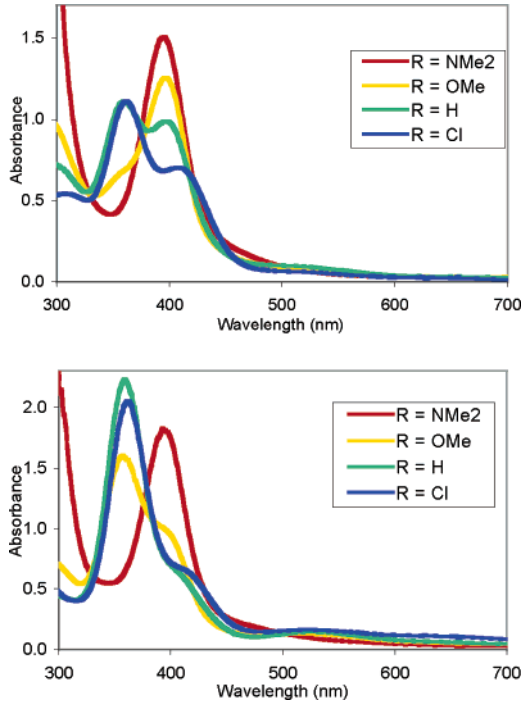


**Figure 4.** Absorbance spectra of the oxygenation reaction of $\mathbf{1^R}$ in THF (top) and $CH_2Cl_2$ (bottom) at −78 °C. All at a similar concentration of ~0.4 mM in THF or ~0.5 mM in $CH_2Cl_2$.

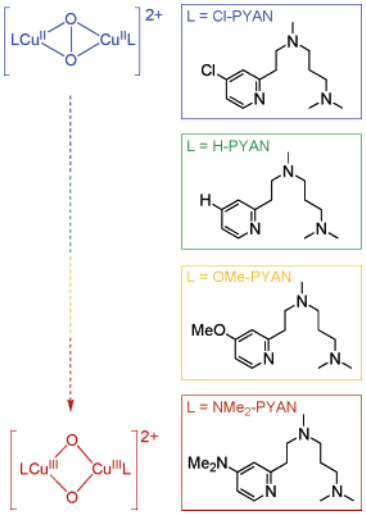


**Figure 5.** Shift in equilibrium from $[Cu^{II}_2(O_2)]^{2+}$ to $[Cu^{III}_2(O)_2]^{2+}$ by ligand electronic effects.

bottom). In the noncoordinating $CH_2Cl_2$ solvent, $\mathbf{1^{Cl}}$ and $\mathbf{1^H}$ react with $O_2$ at −78 °C to yield predominantly the side-on peroxo species, $\mathbf{2^{Cl}}$ and $\mathbf{2^H}$, respectively. The dioxygen adduct of the electron-donating complex $\mathbf{1^{OMe}}$ which favors the bis-$\mu$-oxo structure in THF, generates mostly the side-on peroxo structure in $CH_2Cl_2$ with a minor percentage of the bis-$\mu$-oxo species in equilibrium (i.e., $[\mathbf{2^{OMe}}] > [\mathbf{3^{OMe}}]$). The reaction of $\mathbf{1^{NMe2}}$ with $O_2$ does not change even in the noncoordinating solvent and gives exclusively the high-valent dicopper(III) isomer, $\mathbf{3^{NMe2}}$, signifying that pure electronic effects, and not a solvent effect, influences the full formation of the bis($\mu$-oxo) species. Solvent plays a secondary role, specifically in the equilibria between $\mathbf{2^R} \rightarrow \mathbf{3^R}$, where R = Cl, H, and OMe, but the electronic effect takes precedence

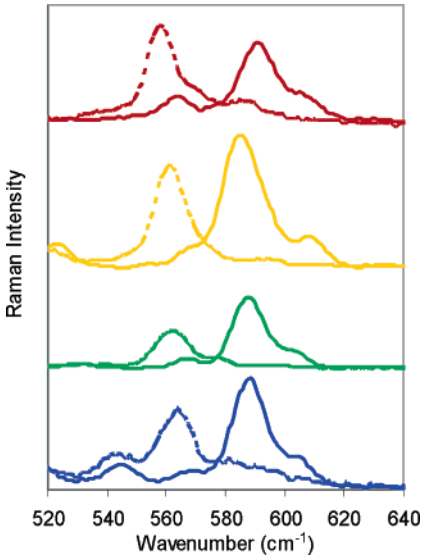


**Figure 6.** rR spectra of $\mathbf{3^R}$ with $^{16}O_2$ (solid lines) and $^{18}O_2$ (dashed lines) for R = $NMe_2$ (red), OMe (orange), H (green), and Cl (blue).

**Table 3.** Resonance Raman Stretching Frequencies ($cm^{-1}$) of Peroxo ($\mathbf{2^R}$) and bis($\mu$-oxo) ($\mathbf{3^R}$) in THF-$d_8$

| | side-on peroxo dicopper(II) | | | | | bis($\mu$-oxo) dicopper(III) | | | |
|---|---|---|---|---|---|---|---|---|---|
| | $\nu$(O−O)[a] | | | | | $\nu(Cu_2O_2)$[c] | | | |
| | $^{16}O_2$ | $^{18}O_2$ | $\Delta\nu$ | $\nu$(Cu−Cu)[b] | | $^{16}O_2$ | $^{18}O_2$ | $\Delta\nu$ |
| $\mathbf{2^{NMe2}}$ | *d* | *d* | *d* | *d* | $\mathbf{3^{NMe2}}$ | 591 | 558 | *f* |
| $\mathbf{2^{OMe}}$ | *e* | *e* | *e* | 287 | $\mathbf{3^{OMe}}$ | 585 | 561 | *f* |
| $\mathbf{2^H}$ | 714 | 678 | −36 | 282 | $\mathbf{2^H}$ | 587 | 562 | *f* |
| $\mathbf{2^{Cl}}$ | 726 | 685 | −41 | 278 | $\mathbf{3^{Cl}}$ | 588 | 564 | *f* |

[a] $\lambda_{ex}$ = 514 nm, $T$ = 195 K. [b] $\lambda_{ex}$ = 364 nm, $T$ = 77 K. [c] $\lambda_{ex}$ = 407 nm, $T$ = 77 K. [d] No $\mathbf{2^{NMe2}}$ features observed nor expected (UV−vis criterion). [e] Attempts to obtain $\nu$(O−O) for $\mathbf{2^{OMe}}$ were unsuccessful due to sample instability at 195 K. [f] Absolute isotope shifts are difficult to evaluate due to Fermi shifting in the $^{16}O_2$ data.

for R = $NMe_2$ since $\mathbf{3^{NMe2}}$ is the sole oxygenation product formed in either THF or $CH_2Cl_2$; also $\mathbf{2^{Cl}}$ is less solvent dependent, as mostly $\mathbf{2^{Cl}}$ is produced in either solvent. Hence, in $CH_2Cl_2$, the equilibrium between a dicopper(II) side-on peroxo and a dicopper(III) bis($\mu$-oxo) species can be tailored to either limit by way of the electron donating/withdrawing R substituent in the ligand system R-PYAN. The low-temperature oxygenation reactions of $\mathbf{1^R}$ were also carried out in acetone and produced similar results to those observed in THF (see Supporting Information).

**Resonance Raman Spectroscopy.** Resonance Raman spectroscopy supports the copper−dioxygen structural assignments derived from the UV−vis absorption data. In THF-$d_8$ with 407 nm excitation, $[\{Cu(R\text{-}PYAN)\}_2(^{16}O_2)]^{2+}$ produces a characteristic dicopper(III) bis($\mu$-oxo) spectrum with a resonance-enhanced peak at ~587 $cm^{-1}$ which shifts by ~25 $cm^{-1}$ when $^{18}O_2$ is used as the dioxygen source (Figure 6).[24,50] The core bis($\mu$-oxo) ($Cu_2O_2$) stretching frequency for $\mathbf{3^R}$ shifts as R is varied; $\nu(Cu_2{}^{16}O_2)$ = 588, 587, and 585 $cm^{-1}$, for R = Cl, H and OMe, respectively (Table 3). The $^{16}O_2$-derived peaks are complicated by Fermi interactions

(50) Holland, P. L.; Cramer, C. J.; Wilkinson, E. C.; Mahapatra, S.; Rodgers, K. R.; Itoh, S.; Taki, M.; Fukuzumi, S.; Que Jr., L.; Tolman, W. B. *J. Am. Chem. Soc.* **2000**, *122*, 792−802.

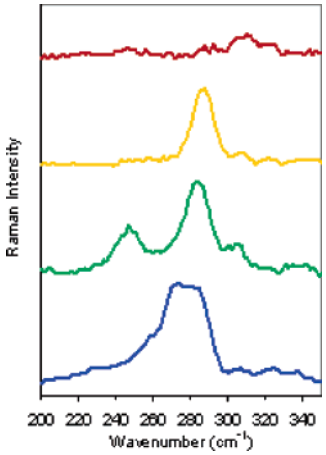


**Figure 7.** rR spectra of $\mathbf{2^R}$ depicting the "Cu−Cu" motion for R = $NMe_2$ (red), OMe (orange), H (green), and Cl (blue).

with peaks in the ~580−600 $cm^{-1}$ region. The $^{18}O_2$-related peaks are shifted out of this region and show a trend of decreasing values with better R donor, shifting from 564 to 562, 561, and 558 $cm^{-1}$ as R changes from Cl to H, OMe, and $NMe_2$, respectively (Table 3). Alternatively, excitation at 364 nm in a THF-$d_8$ solution enhances the side-on peroxo Cu−Cu stretching vibration, $\nu$(Cu−Cu). As R becomes more electron donating (Figure 7), $\nu$(Cu−Cu) shifts to higher frequency, from 278 to 282 to 287 $cm^{-1}$ for $\mathbf{2^{Cl}}$, $\mathbf{2^H}$, and $\mathbf{2^{OMe}}$, respectively.

While the core stretching frequencies for $\mathbf{2^R}$ and $\mathbf{3^R}$ are only modestly affected by the R substituent on the pyridyl nitrogen donor, the O−O stretches of $\mathbf{2^{Cl}}$ and $\mathbf{2^H}$ (in acetone at 514 nm excitation) reveal a significant shift in frequency from $\nu$(O−O) = 726 $cm^{-1}$ for $\mathbf{2^{Cl}}$ to 714 $cm^{-1}$ for $\mathbf{2^H}$ (see Supporting Information).[27] (Note that $\nu$(O−O) could not be obtained for R = MeO and $NMe_2$ due to their dominant conversion to the bis($\mu$-oxo) species and the relatively weak enhancement of $\nu$(O−O) compared to $\nu$(Cu−Cu).) Typical O−O stretching frequencies lie in the 730−760 $cm^{-1}$ range, and only one other example of side-on peroxo complex with a lower $\nu$(O−O) value than 714 $cm^{-1}$ (for $\mathbf{2^H}$)[27] exists.[5,25] The unusually low O−O stretching frequency of $\mathbf{2^H}$ reflects the propensity of that O−O bond to cleave.[24] Indeed, the bond becomes weaker in $\mathbf{2^H}$ relative to $\mathbf{2^{Cl}}$ until it is fully cleaved in $\mathbf{3^{NMe2}}$. Thus, we observe for the first time ligand electronic effects leading to a weakening of $\nu$(O−O) and correlating to corresponding shift in equilibrium from side-on peroxo to bis($\mu$-oxo).

These results are in contrast to those observed for copper complexes of R-MePY2, where increased electron donation from the ligand led to a more limited increase in bis($\mu$-oxo) formation, and had virtually no effect on $\nu$(Cu−Cu) or $\nu$-(O−O).[41] This was attributed to opposing effects, whereby the added electron donation to the copper from the R-MePY2 ligand resulted in a more negatively charged peroxide that hindered back-bonding into the peroxide $\sigma^*$ orbital. Thermodynamic stabilization of the bis($\mu$-oxo) relative to the side-on peroxo with better R donors led to varying mixtures $Cu^{II}_2(O_2)$ and $Cu^{III}_2(O)_2$ coexisting in equilibrium but in all cases favoring the side-on peroxo dicopper(II) isomer.

**Table 4.** Exogenous Substrate Reactivity of $\mathbf{2^H}$ and $\mathbf{3^{NMe2}}$

| | $\mathbf{2^H}$ | $\mathbf{3^{NMe2}}$ |
|---|---|---|
| benzyl alcohol | | |
| → benzaldehyde | 85% | 96% |
| dihydroanthracene | | |
| → anthracene | 81% | 28% |
| → anthrone | [a] | 14% |
| → anthraquinone | [a] | 20% |
| dimethylaniline | | |
| → methylaniline {+ $CH_2(O)$} | 64% | 58% |
| phenylmethyl sulfide | | |
| → phenylmethyl sulfoxide | 52% | 58% |

[a] Negligible amounts detected.

However, the R-PYAN system is significantly different in that, unlike the partial equilibrium shift observed in the $Cu_2O_2$ complexes of R-MePY2, the R-PYAN ligand induces a nearly complete shift from a side-on peroxo dicopper(II) to a bis($\mu$-oxo) dicopper(III) species. This difference in behavior between the two ligand systems might be explained by the second alkyl nitrogen ($N_{alkyl}$) donor present in R-PYAN (R-MePY2 contains two pyridyl donors ($N_{py}$) and only one $N_{alkyl}$ donor) (Chart 1). Alkyl nitrogen donors have been shown to support high-valent dicopper(III) bis($\mu$-oxo) cores by way of $\sigma$ donation to the Cu ion.[19,24] This shift from side-on peroxo to mostly bis($\mu$-oxo) (in the present R-PYAN system) is observed in conjunction with a weakening of the O−O bond. Additional studies are under way to elucidate the fundamental differences in ligand−copper(II) bonding for tridentate amine systems.

**Reactivity of $\mathbf{2^H}$ and $\mathbf{3^{NMe2}}$ toward External Substrates.** The ability to synthesize discrete $[Cu^{II}_2(O_2^{2-})]^{2+}$ and $[Cu^{III}_2(O^{2-})_2]^{2+}$ compounds is desirable for the study of the reactivity patterns of each individual isomeric core. Thus, the reactivity of $[\{Cu(H-PYAN)\}_2(O_2)]^{2+}$ ($\mathbf{2^H}$) as a predominate side-on peroxo dicopper(II) complex and $[\{Cu(NMe_2-PYAN)\}_2(O)_2]^2$ ($\mathbf{3^{NMe2}}$) as a bis($\mu$-oxo) dicopper(III) species toward exogenously added substrates (10-fold excess) was examined (Table 4). Benzyl alcohol, dimethylaniline, and thioanisole were all oxidized/oxygenated, with the product yields not varying too much between $\mathbf{2^H}$ or $\mathbf{3^{NMe2}}$ (Table 4). However, the reaction toward dihydroanthracene varies significantly with the isomers $\mathbf{2^H}$ and $\mathbf{3^{NMe2}}$, the former producing an 81% yield of anthracene, with only 28% observed for $\mathbf{3^{NMe2}}$. However, other over-oxidized products were found, anthrone (14% yield) and anthraquinone (20% yield). While such behavior is known by other strong inorganic metal oxidants,[51,52] the reaction is unprecedented for dicopper−dioxygen species. When $^{18}O_2$ was used as the dioxygen source, according to the intensities of the relevant mass spectrometric peaks, $C_{14}H_8{}^{18}O_2$ (anthraquinone) is observed in 42% yield, and the mixed-labeled and $^{16}O_2$ products, $C_{14}H_8{}^{16}O^{18}O$ and $C_{14}H_8{}^{16}O_2$, are observed in smaller quantities of 31% and 27%, respectively. The low yield of $^{18}O_2$ incorporation may indicate that the over-oxidation may be occurring during the workup process and not from the

(51) Lam, W., W. Y.; Yiu, S.-M.; Douglas, T. Y. Y.; Lau, T.-C.; Yip, W.-P.; Che, C.-M. *Inorg. Chem.* **2003**, *42*, 8011−8018.
(52) Wang, K. M.; James M. *J. Am. Chem. Soc.* **1997**, *119*, 1470−1471.

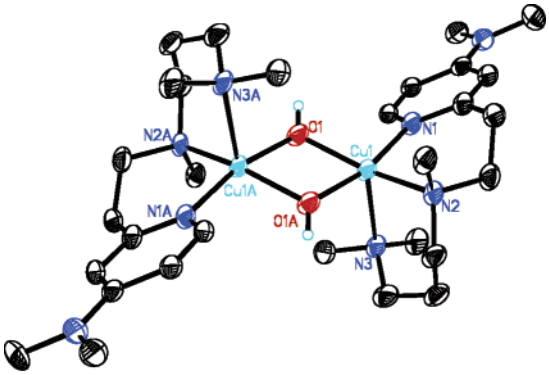


**Figure 8.** Cationic portion of $[\{Cu(NMe_2\text{-}PYAN)\}_2(OH)_2][B(C_6F_5)_4]_2$ ($\mathbf{4^{NMe2}}$) at the 50% probability level.

actual dicopper−dioxygen adducts; further studies are needed.

Based on yields, differential reactivity of the different dicopper cores ($\mathbf{2^H}$ and $\mathbf{3^{NMe2}}$) does not seem apparent. However, preliminary observations show that the side-on peroxo $\mathbf{2^H}$ and bis($\mu$-oxo) $\mathbf{3^{NMe2}}$ react with thioanisole at considerably different rates: the reaction by $\mathbf{2^H}$ is over in less than 1 h, but oxidation by $\mathbf{3^{NMe2}}$ takes ~20 h (under similar reaction conditions/concentrations). Further, the oxidation of benzyl alcohol takes twice as long when $\mathbf{3^{NMe2}}$ is used as the oxidant compared to $\mathbf{2^H}$, and most interestingly, the oxidation of dimethylaniline by $\mathbf{2^H}$ and $\mathbf{3^{NMe2}}$ appears to occur via different kinetic mechanisms.[53] While these are currently only general observations, they indicate that rich, mechanistic insights may be obtained in future studies on the oxidative chemistry of the distinctive side-on peroxo ($\mathbf{2^H}$) and bis($\mu$-oxo) ($\mathbf{3^{NMe2}}$) cores.

**Bis($\mu$-OH) Dicopper(II) Compounds ($\mathbf{4^R}$).** In the absence of external substrates, or upon warming, the dioxygen intermediates $\mathbf{2^R}$ and $\mathbf{3^R}$ transform to stable bis($\mu$-OH) dicopper(II) compounds ($\mathbf{4^R}$) analogous to the decomposition products of $[\{Cu(R\text{-}MePY2)\}_2(O_2)]^{2+}$ and many other dicopper−dioxygen intermediates.[40,47] The $\mathbf{4^R}$ thermal decomposition products were characterized by UV−vis and IR spectroscopy with $[\{Cu(NMe_2\text{-}PYAN)\}_2(OH)_2][B(C_6F_5)_4]_2$ ($\mathbf{4^{NMe2}}$) also being analyzed by X-ray crystallography (Figure 8).

The dihydroxy structure shows that the pyridyl- and central-amine donors bind equatorially and the peripheral amine coordinates axially, at least in this structure. Whether or not this same ligand wrapping likely occurs around the $Cu^{II}$ centers in $\mathbf{2^R}$ and $\mathbf{3^R}$ will be assessed in a future report. The structure of $\mathbf{4^{NMe2}}$ contains a center of symmetry, and the copper(II) centers adopt a distorted square pyramidal geometry where the axial ligands are anti with respect to one another. According to Addison and Reedijk's description for five-coordinate centric molecules,[54] the central copper atoms deviate from perfect square pyramidal form with $\tau = 0.19$, a distortion larger than the $Cu^{II}_2(\mu\text{-}OH)_2$ analogue supported by the ligand $NMe_2$-MePY2.[55] We surmise that this may a consequence of the asymmetry of the $NMe_2$-PYAN ligand.

(53) The overall reaction order is different for $\mathbf{2^H}$ and $\mathbf{3^{NMe2}}$.
(54) Addison, A. W.; Rao, T. N.; Reedijk, J.; van Rijn, J.; Verschoor, G. C. *J. Chem. Soc., Dalton Trans.* **1984**, 1349−1356.

**Table 5.** Spectroscopic and Physical Properties of $\mathbf{4^R}$

| | UV−vis [nm ($M^{-1}$ $cm^{-1}$)] | $\nu$(O−H) ($cm^{-1}$) | $\mu$-eff [B.M./$Cu^{II}$] |
|---|---|---|---|
| $\mathbf{4^{NMe2}}$ | 670 (380) | 3651 | 1.2 |
| $\mathbf{4^{OMe}}$ | 680 (300) | 3655 | 1.6 |
| $\mathbf{4^H}$ | 670 (380) | 3653 | 1.3 |
| $\mathbf{4^{Cl}}$ | 670 (360) | 3649 | 1.2 |

The thermal transformation product $\mathbf{4^{NMe2}}$ is also characterized by its $Cu^{II}$ d−d transitions at $\lambda_{max} = 670$ nm (380 $M^{-1}$ $cm^{-1}$) and a sharp O−H infrared stretch at 3651 $cm^{-1}$ (Table 5). The corresponding products $\mathbf{4^{OMe}}$, $\mathbf{4^H}$, and $\mathbf{4^{Cl}}$ have similar spectroscopic properties to those of crystalline $\mathbf{4^{NMe2}}$, with d−d transitions at 680 (300 $M^{-1}$ $cm^{-1}$), 670 (380 $M^{-1}$ $cm^{-1}$), and 670 nm (360 $M^{-1}$ $cm^{-1}$), and sharp O−H stretches at 3655, 3653, and 3649 $cm^{-1}$, for $\mathbf{4^{OMe}}$, $\mathbf{4^H}$, and $\mathbf{4^{Cl}}$, respectively. The room-temperature magnetic properties of $\mathbf{4^R}$ were determined by the Evans method[56] and values of 1.2, 1.6, 1.3, and 1.2 $\mu_B$ per $Cu^{II}$ ion were found for the complexes with R = $NMe_2$, OMe, H, and Cl, respectively. These are diminished $\mu_{eff}$ values relative to that for typical $d^9$ $Cu^{II}$ complexes ($\mu_B \geq 1.73$, but usually >2.0), but are typical for a dihydroxy bridged antiferromagnetically coupled dicopper(II) core. A summary of the physical properties of $\mathbf{4^R}$ is presented in Table 5.[47]

## Summary and Conclusions

This study further evaluates the factors affecting the equilibrium between a $\mu$-$\eta^2$:$\eta^2$-(side-on)-peroxo dicopper(II) species and its bis($\mu$-oxo) dicopper(III) complex isomeric form. We have showed that seemingly small changes in the electronic environment around the copper(I) center can drastically influence the structure of the resulting $Cu_2O_2$ adduct. While the pyridyl substituent only marginally affects the $Cu^{II}/Cu^{I}$ redox couple and the back-bonding to CO in $[Cu^{I}(R\text{-}PYAN)(CO)]^+$, it is capable of shifting the equilibrium from a dicopper complex that is mostly the side-on peroxo isomer to the bis($\mu$-oxo) extreme for R = $NMe_2$. A significant electronic effect is observed; O−O bond weakening occurs with a ligand which is a better donor; the O−O bond stretch decreases from 726 $cm^{-1}$ in $\mathbf{2^{Cl}}$ to 714 $cm^{-1}$ in $\mathbf{2^H}$. It is noteworthy that, while the complexes of R-MePY2 exhibit larger differences in CO stretches and $Cu^{II}/Cu^{I}$ reduction potentials, the dioxygen reactivity is only moderately affected. One might have expected a larger electronic effect from the copper(I) complexes of R-MePY2 rather than with those with R-PYAN due to the double substituent effect arising from the second pyridyl arm. One key difference possibly leading to the variations between the two systems is the nature of the nitrogen donors of the chelating ligand. Alkylamine ligands are better $\sigma$ donors to the copper ion and are able to stabilize a high-valent dicopper(III) core.[24] R-PYAN contains two alkylamine ligand donors, versus just one alkylamine nitrogen in R-MePY2. It may be this feature that apparently allows the R-PYAN system of copper−dioxygen adducts to lie close to the midpoint (i.e., 1:1 ratio of concentrations) of the peroxo/bis($\mu$-oxo) equilibrium and

(55) Zhang, C. X. Ph.D. Dissertation, Johns Hopkins University, 2001.
(56) Evans, D. F. *J. Chem. Soc.* **1959**, 2003.

to truly probe how small electronic modifications can cause very clearly measurable effects on the copper−dioxygen chemistry which must be arising only from the R variations of the R-PYAN pyridyl donor. Indeed, ligand electronic effects can be a significant contributions to the side-on peroxo/bis($\mu$-oxo) equilibrium.

Finally, both dicopper cores can oxidize external substrates in reasonable yields, allowing for a further investigation of the reactivity patterns of each $Cu^{II}_2(O_2)$ and $Cu^{III}_2(O)_2$ isomers without introducing drastic changes in the supporting ligand. The preliminary overview reactivity studies presented here qualitatively show differential oxidative reactivity according to reaction kinetics. Future studies will focus on uncovering detailed mechanistic insights in order better understand the oxidative chemistry of (side-on)-peroxo dicopper(II) versus bis($\mu$-oxo) dicopper(III) species.

**Acknowledgment.** K.D.K (GM28962) and E.I.S. (DK31-450) are grateful to the National Institutes of Health for financial support of this research. We also thank Dr. Liviu M. Mirica for his assistance in resonance Raman sample preparation.

**Supporting Information Available:** X-ray crystallographic data in cif format and supplemental figures. This material is available free of charge via the Internet at http://pubs.acs.org.

IC052185M